



## Supporting Information

© Copyright Wiley-VCH Verlag GmbH & Co. KGaA, 69451 Weinheim, 2019

### **New Oleic Acid-Capped Mesoporous Silica Particles as Surfactant-Responsive Delivery Systems**

Elisa Poyatos-Racionero, Édgar Pérez-Esteve, M. Dolores Marcos,\* José M. Barat, Ramón Martínez-Máñez,\* Elena Aznar, and Andrea Bernardos© 2019 The Authors. Published by Wiley-VCH Verlag GmbH & Co. KGaA. This is an open access article under the terms of the Creative Commons Attribution Non-Commercial NoDerivs License, which permits use and distribution in any medium, provided the original work is properly cited, the use is non-commercial and no modifications or adaptations are made.

### General techniques for characterization

Powder X-ray diffraction (PXRD), transmission electron microscopy (TEM), N<sub>2</sub> adsorption-desorption, thermogravimetric analysis (TGA), elemental analysis, Dynamic Light Scattering (DLS),  $\zeta$  potential, UV-visible (UV-vis) and fluorescence spectroscopy were employed to characterize synthesized materials. PXRD measurements were taken on a D8 Advance diffractometer using CuK $\alpha$  radiation (Philips, Amsterdam, The Netherlands). TEM images were obtained with a 100 kV CM10 microscope (Philips). N<sub>2</sub> adsorption-desorption isotherms were recorded with a Tristar II Plus automated analyzer (Micromeritics, Norcross, GA, USA). The samples were degassed at 120 °C in vacuum overnight. Specific surface areas were calculated from the adsorption data within the low-pressure range using the Brunauer, Emmett and Teller (BET) model. Pore size was determined following the Barret, Joyner and Halenda (BJH) method. Thermogravimetric analyses were carried out on a TGA/SDTA 851e balance (Mettler Toledo, Columbus, OH, USA) in an oxidizing atmosphere (air, 80 mL min<sup>-1</sup>) with a heating program which consist of a gradient of 393-1273 K at 10 °C min<sup>-1</sup>, followed by an isothermal heating step at 1273 °C for 30 min.  $\zeta$  potential of the particles was measured in Ethanol 96% at 20 °C by Zetasizer Nano ZS equipment (Malvern Instruments, Malvern, UK) and their size was measured by DLS in a Malvern Mastersizer 2000 (Malvern Instruments, Malvern, UK). Fluorescence spectroscopy measurements were taken on a JASCO FP-8500 fluorimeter and UV-Visible spectra were recorder with a JASCO V-650 spectrophotometer.

### Chemicals

Tetraethylortosilicate (TEOS), Pluronic 123 (P123), Hydrochloric acid 37% (HCl), N-cetyltrimethylammonium bromide (CTABr), (3-Aminopropyl)triethoxysilane (APTES), N-(3-Dimethylaminopropyl)-N'-ethylcarbodiimide (EDC), N,N'-Dicyclohexylcarbodiimide (DCC), Rhodamine B (RhB), oleic acid, the employed surfactants (SDS, LAS, Triton™- X100), all the chemicals for the digestive fluids (bile extract included) and enzymes (pancreatin, pronase, pepsin and esterase) were provided by Sigma (Sigma-Aldrich Química S.L., Madrid, Spain). Riboflavin 5-Phospate was provided from Proquimac (Barcelona, Spain); and ethanol (extra pure and 96%), methanol and acetone were purchased from Scharlau (Barcelona, Spain). Bile extract from Sigma Aldrich had bile salts concentration between 3 and 8 × 10<sup>-3</sup> M.

### Mesoporous silica particles synthesis

SBA-15 microparticles were synthesized following the method described by Zhao et al.<sup>1</sup> P123 was used as structure-directing agent. Molar ratio of the reagents was fixed to 0.017 P123:1.0 TEOS:6 HCl:196 H<sub>2</sub>O. The preparation was performed by mixing an aqueous solution of 4 g of P123 with HCl 37%, and stirring for 2 h, after which the silica source, TEOS, was added dropwise. This final mixture was stirred for a further 24 h, and it was aged in an autoclave at 100 °C for 24 h. The mixture was filtered, the obtained white solid was washed with deionized water until neutral pH and dried at 70 °C overnight. The final SBA-15 particles were obtained by calcination of the as-synthesized solid at 550 °C during 5 h in oxidant atmosphere with the aim of removing the surfactant template.

### Characterization

All the solids were characterized using standard techniques, as powder X-Ray diffraction (PXRD), transmission electron microscopy (TEM), N<sub>2</sub> adsorption-desorption isotherms (N<sub>2</sub> ads-des), thermogravimetric analysis (TGA) and elemental analysis (EA).

The PXRD (Figure S1 a-d) of all solids show a sharp peak and two minor ones indexed as (100), (110) and (200) Bragg reflections, respectively, indicating that the porous structure is preserved during the loading and functionalization processes. The mesoporous structure of all the solids was confirmed from TEM analysis, in which the typical channels of the SBA-15 matrix were visualized as alternate black and white stripes (see Figure S1 e-g for TEM images of solids **S0** and **S2**, and **S3** respectively).

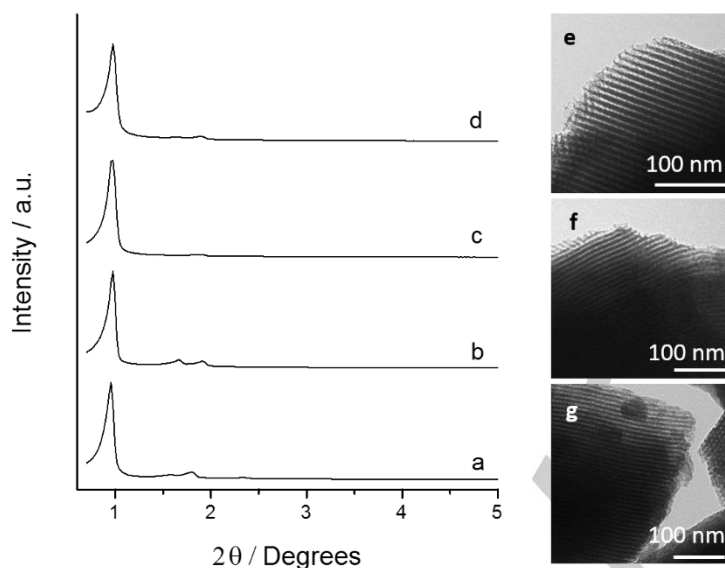


**Figure S1.** Left: powder X-ray diffraction (PXRD) patterns of solids (a) SBA-15 particles as made, (b) SBA-15 calcined and (c) **S2**, (d) **S3** Right: TEM images of (e) SBA-15 calcined, (f) **S2** and (g) **S3**, showing the typical porosity of the mesoporous silica matrix.

The  $N_2$  adsorption-desorption isotherms of the microparticles SBA-15 calcined material is shown in Figure S2. A typical curve for these mesoporous solids consisting of an adsorption step at intermediate  $P/P_0$  value (0.1-0.3) can be observed. This curve corresponds to a type IV isotherm, in which the observed step corresponds with nitrogen condensation inside the mesopores. The pore diameter (5.3 nm) and pore volume ( $0.82 \text{ cm}^3 \text{ g}^{-1}$ ) values were calculated using the BJH model on the adsorption branch of the isotherm. The application of the BET model resulted in a value of  $678.6 \text{ m}^2/\text{g}$  for the total specific surface (**Table S1**).

The  $N_2$  adsorption-desorption isotherm of solids **S2** and **S3** is typical of mesoporous systems with practically filled mesopores (see Figure S2). Consequently, relatively low  $N_2$  adsorbed volume and surface area (see **Table S1**) values were calculated. In fact, these solids show flat or almost flat curves when compared to those of the SBA-15 parent material, which indicates significant pore blocking and the subsequent absence of appreciable mesoporosity.

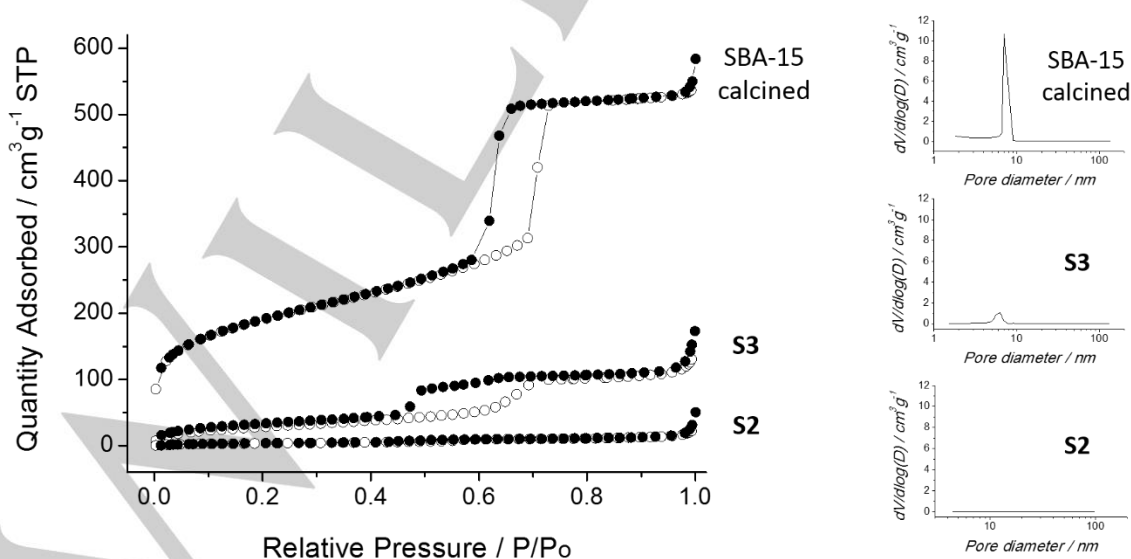


**Figure S2.** Left: nitrogen adsorption (O) – desorption (●) isotherms for SBA-15 mesoporous materials: SBA-15 calcined (top), loaded and functionalized solid **S3** (middle) and loaded and functionalized solid **S2** (bottom). Right: pore volumes of SBA-15 calcined, **S3** and **S2** (top, middle and bottom, respectively).

**Table S1.** BET specific surface values, pore volumes and pore sizes calculated from the N<sub>2</sub> adsorption-desorption isotherms for selected materials.

	S <sub>BET</sub> (m <sup>2</sup> g <sup>-1</sup> )	Pore Volume <sup>a</sup> (cm <sup>3</sup> g <sup>-1</sup> )	Pore size <sup>a</sup> (nm)
calcined SBA-15	678.6	0.82	5.32
<b>S2</b>	14.3	0.03	-
<b>S3</b>	108.0	0.19	-

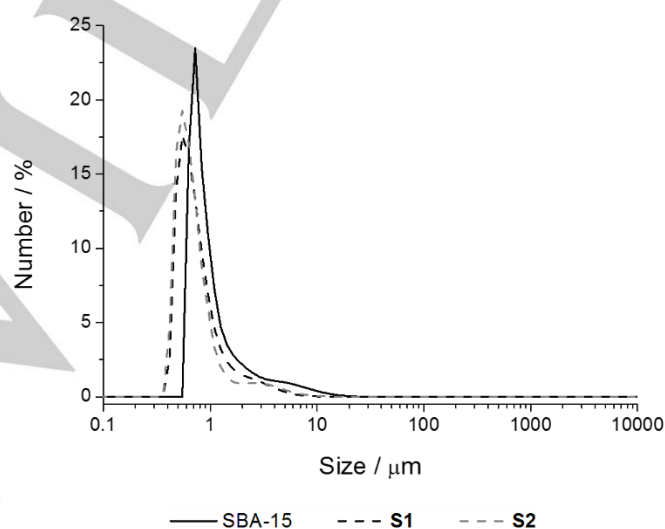
<sup>a</sup>Pore volumes and pore sizes were estimated by using the BJH model applied on the adsorption branch of the isotherm. Data were restricted to intraparticle mesopores.

Thermogravimetric analysis (TGA) and elemental analysis (EA) indicated an organic matter content of 43.1 mg RhB g<sup>-1</sup> SiO<sub>2</sub> and 84.7 mg molecular gate g<sup>-1</sup> SiO<sub>2</sub> in **S2**; and 50.0 mg Riboflavin-5P g<sup>-1</sup> SiO<sub>2</sub> and 167.2 mg molecular gate g<sup>-1</sup> SiO<sub>2</sub> in **S3**. The proportion in mmol of all the moieties is summarized in Table S2.

**Table S2.** Content of RhB/Riboflavin-5P, APTES and oleic acid in the solids **S2** and **S3**.

Solid	α <sub>RhB</sub> (mmol g <sup>-1</sup> SiO <sub>2</sub> )	α <sub>APTES</sub> (mmol g <sup>-1</sup> SiO <sub>2</sub> )	α <sub>Oleic acid</sub> (mmol g <sup>-1</sup> SiO <sub>2</sub> )
<b>S2</b>	0.09	1.23	0.08
<b>S3</b>	0.11	1.09	0.40

The size of the particles was measured in ethanol 96%. A distribution of particles between 0.5 and 5 μm (mainly 1 μm) was obtained. The functionalization process gave smaller particles' size due to the repulsion effect between the charged moieties around the material's surface, which avoids the aggregation between particles (see Fig S3).

**Figure S3.** Size distribution of solids SBA-15, **S1** and **S2**.

Infrared spectroscopy and  $\zeta$  potential were also used for following the functionalization process leading to solids **S2** and **S3**. In all the FTIR spectra the dominant bands are those due to the silica matrix (1060, 790 and 450  $\text{cm}^{-1}$ ). However, some changes in minor bands can be related with the presence of functionalized groups in solids **S2** and **S3**. Thus, it is possible to observe the decrease of the band at 960  $\text{cm}^{-1}$  assignable to the silanol group vibration when the APTES group is anchored to the surface of the silica matrix. Also it is visible the appearance two bands at 2930  $\text{cm}^{-1}$  and 2850  $\text{cm}^{-1}$  assignable to the bending C–H vibrations, that increase as the functionalization process proceeds (see Figure S4). On the other hand, the region that would have told us about the formation of the amide group shows an important number of bands due to the complex structure of the loaded molecules. Though it is difficult to unambiguously assign the bands between 1700  $\text{cm}^{-1}$  and 1250  $\text{cm}^{-1}$  many changes can be observed with the functionalization process as for example the decrease of the bands at 1330  $\text{cm}^{-1}$  and 1270  $\text{cm}^{-1}$  that could be assigned to the C–N vibration of the propylamine when anchoring the oleic acid to get the final gating moiety.

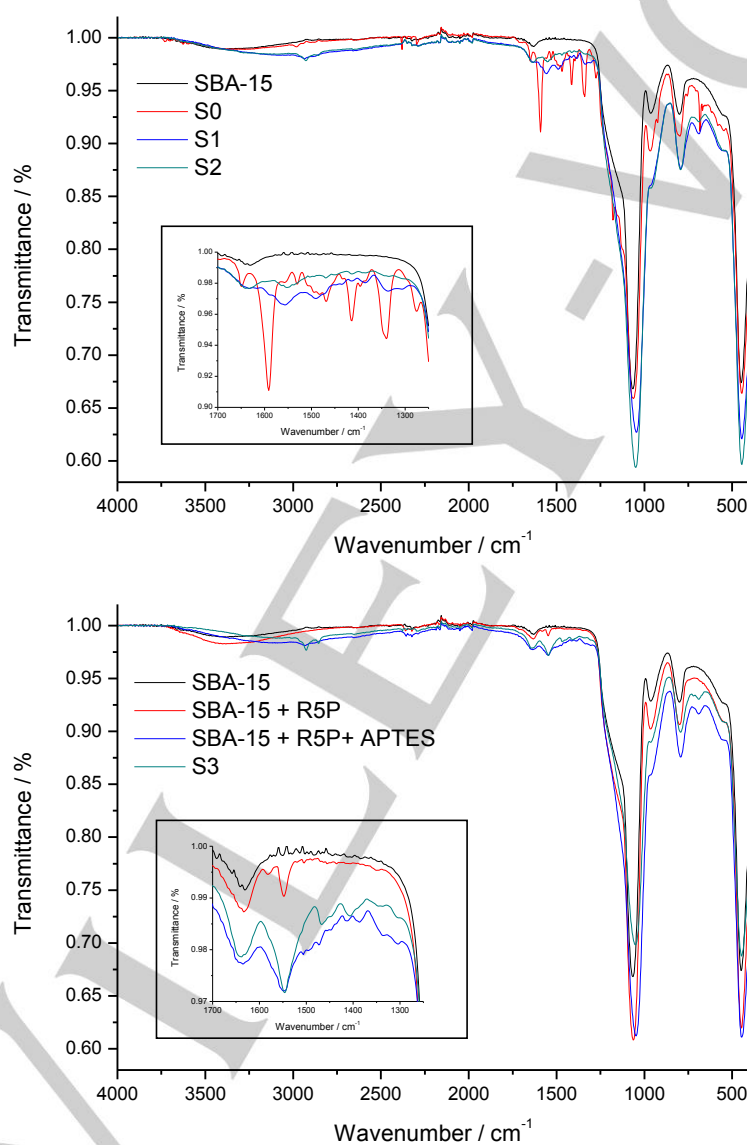


**Figure S4.** Top: Infrared spectra of the synthesis process of solids with RhB (**S0**, **S1**, **S2**). Bottom: Infrared spectra of the synthesis process of solids with Riboflavin-5P (SBA-15 + Riboflavin-5P, SBA-15 + Riboflavin-5P + APTES, **S3**).

$\zeta$  potential values are in agreement with the expected values for the external moieties. The starting material SBA-15 has a negative value of -27.45 mV which is still negative when the solids are loaded (**S0** and SBA-15 + Riboflavin-5P). The value changes to positive when APTES is added, due to the external amine groups (41.48 and 23.68 mV for **S1** and SBA-15 + Riboflavin-5P + APTES, respectively), and the values are still positive when oleic acid is added, due to the amide groups in the surface (see Fig S5).

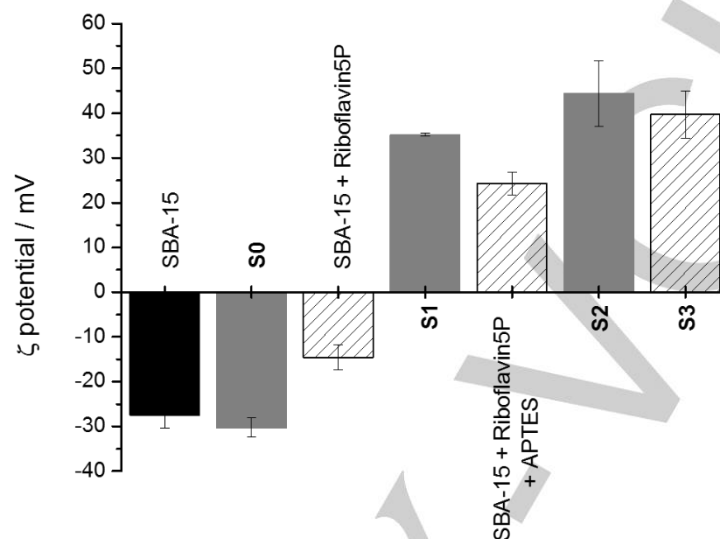


**Figure S5.**  $\zeta$  potential values of the different solids synthesized from SBA-15 (black). The solids loaded with Rhodamine B are represented with solid gray bars, and solids loaded with Riboflavin-5P are represented with white striped bars.

### Cargo release kinetics

In a typical experiment, 5 mg of solid **S2** were placed in 10 mL of PBS, simulating a general aqueous medium, and 10 mL of bile salts suspension (100 mg of bile salts in 10 mL of PBS), simulating conditions at the small intestine. At certain times aliquots were taken and filtered. Delivery of RhB from the pore voids to the different solutions was analyzed via the fluorescence emission band of this molecule at 572 nm (excitation at 555 nm, see Fig S6 left).

The procedure was repeated with some variations for the delivery of riboflavin from solid **S3**. In this experiment, 5 mg of solid **S3** were placed in 10 mL of distilled water and 10 mL of a CTAB  $10^{-2}$  M solution as surfactant (to avoid the redox and pH effects of a complex matrix like bile salts on a sensible molecule like riboflavin-5P). The cargo release profiles are shown in Fig S7. Riboflavin-5P release was followed and quantified by means of its absorption band at 451 nm (see Fig S6 right).

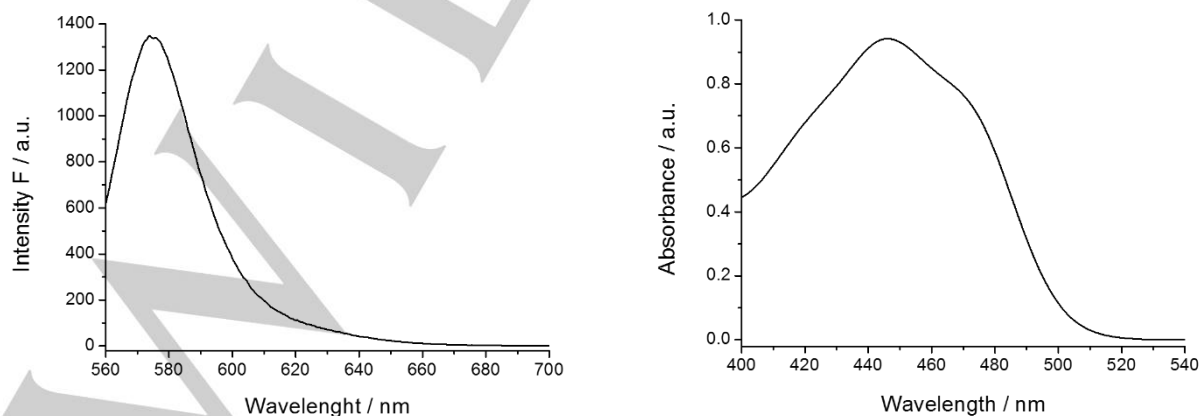


**Figure S6.** Left: fluorescence spectrum of Rhodamine B in water or bile solution. Right: Absorption spectrum of Riboflavin-5P in water or CTAB solution.

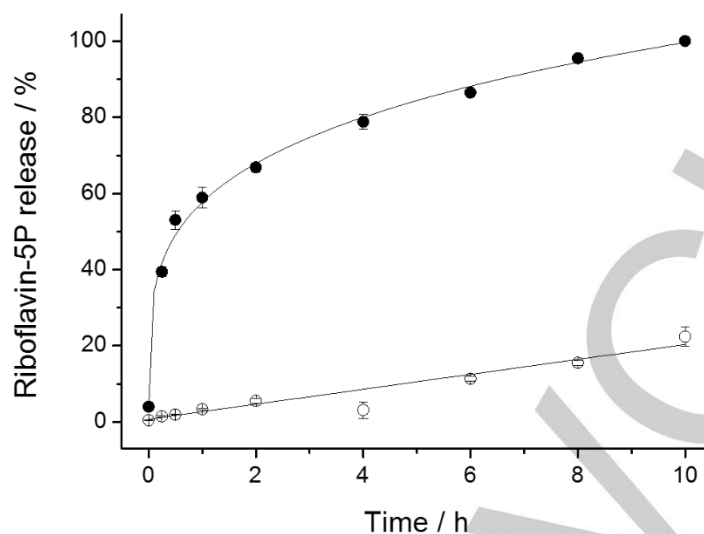


**Figure S7.** Kinetic release profile of riboflavin-5P from solid **S3** in aqueous medium without surfactant molecules ( $\circ$ ), and when CTAB molecules are present ( $\bullet$ ).

### ***In vitro* digestion**

An *in vitro* digestion model consisting of mouth, gastric and intestinal phases was used to simulate the typical chemical composition, pH and residence time periods of each of the three main compartments of the gastrointestinal tract (GIT), in order to monitor the cargo release in the different sections of the GIT.<sup>2</sup> The pH values of the digestive juices were checked and, if necessary, adjusted to the appropriate interval with  $\text{NaHCO}_3$  (1 M) or HCl (37% w/w).

In a typical experiment, 10 mg of solid **S2** were added to three vials (A, B and C) with the specified volume of simulated fluids (saliva, gastric fluid and intestinal fluid respectively). 3 mL of saliva fluid were added to the three vials, and aliquots were taken from vial A. Once the permanence time in the mouth was achieved, 6 mL of gastric fluid were added to vials B and C, and the respective aliquots were taken from vial B. Finally, when the two hours of gastric permanence were completed, 12 mL of intestinal fluid and 1 mL of  $\text{NaHCO}_3$  1M (to adjust the pH value) were added to the last vial, C; and the pertinent aliquots were taken from it.

The aliquots taken at the stipulated times (0 and 5 min for saliva; 0, 15, 30, 60, 90 and 120 min for gastric fluid; and 0, 15, 30, 60, 90, 120 and 180 min for intestinal fluid) were filtered and its fluorescence ( $\lambda_{\text{ex}} = 555 \text{ nm}$ ,  $\lambda_{\text{em}} = 572 \text{ nm}$ ) was measured in order to register the amount of rhodamine B released from the pore voids.

### **REFERENCES**

- [1] D. Zhao, J. Feng, Q. Huo, N. Melosh, G. H. Fredrickson, B. F. Chmelka and G. D. Stucky, *Science.*, 1998, **279**, 548–552.
- [2] C. H. M. Versantvoort, A. G. Oomen, E. Van De Kamp, C. J. M. Rompelberg and A. J. A. M. Sips, *Food Chem. Toxicol.*, 2005, **43**, 31–40.